A Modified Accelerated Chloride Migration Tests for UHPC And UHPFRC With PVA And Steel Fibers

Juliano Provete Vincler, Thomas Sanchez, Vicky Turgeon,

David Conciatori* and Luca Sorelli

Department of water and civil engineering, Laval University Laval, Canada

*Corresponding author. E-mail address: david.conciatori@gci.ulaval.ca

Abstract

Accelerated migration tests which are commonly used to measure chloride diffusion in ordinary cement-based materials cannot be directly applied to composite with very low permeability, such as Ultra High-Performance Fiber Reinforced concretes (UHPFRC). In order to assess the UHPFRC enhancement on the structural durability, there is a critical need to accurately assess the permeability level of the material to chloride ions. The objective of this work is to adapt an existing set-up of accelerated chloride migration test in order to (i) better characterize the resistance of chloride ion penetration in UHPFRC; and (ii) to compare the resistance of chloride ion penetration between UHPC and UHPFRC. The material characterization, the set-up modifications of the existing accelerated migration test, the results are presented. In conclusion, the modification of the test-set-up allowed to accurately measure chloride transport of very low permeability UHPFRC and to shed light on the effect of the fiber reinforcement.

Keywords: UHPC, UHPFRC, chloride, diffusion, profiles, migration test

1. INTRODUCTION

Ultra-High-Performance Concrete (UHPC) and Ultra-High-Performance Fiber Reinforced Concrete (UHPFRC), respectively without and with fibers, were successfully employed for structural applications thanks to their outstanding compressive strength and tensile toughness along with its remarkable durability. UHPFRC improved concrete structures in terms of longer span, material saving, and enhanced lifetime. Decades of research leads to UHPFRC as it is known today, with its low porosity and high-packing density [1]. The outstanding UHPFRC durability is based on their extremely low permeability and diffusivity, which is achieved by maximizing the microstructure packing density [2]–[5]. Thus, external layer of UHPFRC can be effectively employed to enhance both the strength of damaged concrete structure and their permeability to external aggressive agents with an optimal gain in terms of the structure lifetime [6], [7].

One of the major durability issues for reinforced concrete structure is unequivocally the chloride permeability that leads to the corrosion of steel bars [8]–[11]. Very few tests exist on chloride resistance of UHPFRC in real field conditions and this information is key for estimating the economic gain on the maintenance cost and the structure lifetime especially in regions with severe climate conditions [12], [13]. As for example, Thomas et al. monitored the chloride penetration in a material prism without fibers (UHPC) under real field conditions which consists of twice-daily tides of wet/dry cycles and winter freeze/thaw cycles [14]. After a period of about 12-15 years of severe marine exposure, the chloride penetration depth was limited to 6-10 mm, which was approximately one third of the chloride penetration depth observed on reference samples of High-Performance Concrete. As for laboratory tests, different kinds of accelerated tests exist to rapidly assess the chloride ion penetration resistance of

concrete [15]–[18]. Depending on the test method, different types of results can be obtained, such as chloride profile, effective or apparent diffusion coefficient or with a number of Coulomb to give an indicative rank of the chloride ion permeability of the material. These results that can be difficult to compare. Many other factors influence the determination of the chloride ion permeability such as the type of material, the preparation procedure of the specimen or the testing method. These results are then interpreted to judge of the durability of the material regarding the chloride ion penetration. However, such tests may not be suitable to accurately measure the diffusion coefficient of UHPFRC and characterize their durability regarding the chloride ion permeability. In standard test methods, such as ASTM C1202 [19], an electrical field applied accelerate the chloride diffusion. That is difficult to measure the diffusion through samples because of undesirable temperature raise and short-circuit due to favorable alignment of the fibers. In fact, the recent standard for fabricating and testing UHPFRC specimen (ASTM C1856 [20]), specify that the ASTM C1202 test method is not applicable for UHPFRC (including fibers) for the previously mentioned reasons.

Despite the difficulty and uncertainty of the ASTM C1202 test method for UHPC with fibers, some research shows successful tests and concluding results for UHPC with and without fibers. The results, ranging from 0 to 360 Coulombs, correspond to the negligible chloride ion permeability of the standard and no significant difference is observable between UHPC matrix with and without fibers. However, a literature review of the chloride ion permeability of UHPC in terms of apparent diffusion coefficient, which consider chemical interaction with the material, shows great scattering of results. The results are not from accelerated test, that is without electrical current and thus spend much time than accelerated tests. Thomas et al. and Piérard et al. report respectively an apparent diffusion coefficient of $1.3x10^{-13}$ m^2/s and

67 $2x10^{-13}$ m^2/s for UHPC. Tanaka obtain an apparent coefficient of diffusion of $4x10^{-15}$ m^2/s for
68 UHPFRC exposed for 5 years in an open box girder of a bridge and $4.7x10^{-16}$ m^2/s for
69 immersed UHPFRC in chloride solution for 2.5 years. Table 1 shows a summary of the results
70 from the considered research.

REFERENCE	FIBERS	RESULT		TESTING METHODS
Habel et al. [21]	ø	88	Coulomb	ASTM C1202 (6h)
	5.5% steel	72		
Thomas et al. [14]	ø	0, 19		
Bonneau et al. [22]	ø	6, 7		
	140 kg/m^3 PVA	6, 9		
Graybeal [17]	2% steel	18, 18, 26, 39, 76, 360		
Ahlborn et al. [23]	2% steel	15, 75		
Thomas et al. [14]	ø	$1.3x10^{-13}$	Apparent diffusion coefficient (m^2/s)	ASTM C1556 [24] (63d.)
Piérard et al. [25]	ø	$2x10^{-13}$		NT Build 443 [26] (90d.)
Tanaka [27]	2% steel	$4x10^{-15}$		5y. exposure in a bridge
		$4.7x10^{-16}$		2.5y. immersion in chloride solution

71 Table 1. Results of chloride ion penetration resistance from literature

72 While test method ASTM C1202 does not highlight significant difference in result of the
73 chloride ion permeability for UHPC or UHPFRC from the different experiments, a difference
74 can be observed for diffusion coefficients of UHPC and UHPFRC with natural diffusion tests.
75 These results suggest that the ASTM C1202 test method may be insufficient to accurately
76 characterize the chloride ion permeability of UHPFRC and the results on the unique UHPC
77 matrix may not be representative of the real application of the material with fibers. It can
78 therefore lead to strong difference on the lifetime prediction or the optimal design of the steel
79 rebar cover in thin UHPFRC elements [28].

In order to improve the durability design of UHPFRC, this paper aims to propose an alternative test method to ASTM C1202 in order to (i) efficiently characterize the resistance of chloride ion penetration in UHPFRC; and (ii) compare the resistance of chloride ion penetration between UHPC and UHPFRC with two different types of fibers and volume content. Additionally, the effect of different preparation procedure of the specimen on the chloride transport properties was also considered.

2. MATERIALS AND METHODS

2.1 Mix designs and sample preparation

UHPC. The mix is commercially available under the name of Ductal® and composed of 2195 kg/m³ of premix, 35 kg/m³ of superplasticizer type A&F [29] and 125 kg/m³ of water for UHPC. The water-to-binder ratio was about 0.17. UHPC mix was batched in a small Hubert mixer (7 liters) and cast in a polyvinyl chloride cylindrical molds (100 mm diameter and 200 mm height). The sample surface was protected for 24 h with a wet cover before demolding.

UHPFRC-PVA. The water amount of the UHPC mix with polyvinyl alcohol fibers was corrected to 150 kg/m³ to consider the PVA fiber absorption. The water-to-binder ratio is about 0.21 and PVA fibers are 12.0 mm length and 0.2 mm diameter. The fiber volume content was varied between 1%, 2%, 4%, and 5%. The UHPFRC-PVA samples were prepared with the same procedure as for UHPC samples.

UHPFRC-STEEL. The mix UHPC with steel fibers is composed of 125 kg/m³ of water and the water-to-binder ratio is about 0.17 [16]. The average geometry is 12.7 mm length and 0.2 mm diameter for steel fiber. Two casting methods were done for this mix respectively named G1 and G2.

The **G1 group** had fiber volumes content varying between 1%, 2%, 4%, and 5%. Two cylinders for each fiber volume were cast. During placements, the fresh concrete was vibrated, and the fibers were added before the UHPFRC turned fluid thanks to its thixotropic behavior. A slump flow test was carried out. After unmolding, the cylinders were thermally cured for one week according to the following phases: (i) 24 h submersion in lime saturated water at the laboratory temperature of 20 °C; (ii) 48 h curing at the temperature of 60 °C with relative humidity of about 90%; and (iii) 96 h submersion in lime saturated water at laboratory temperature of 20 °C; (iv) curing at 100% relative humidity until the testing day.

For **G2 group**, the steel fiber volume contents were considered from 1% to 4%. Four cylinders for each fiber volume content were cast. No mechanical vibration was applied during the placement and the fibers were added only after the thixotropic matrix fluidification. After unmolding, the cylinders were cured according to the following steps: (i) 96h submersion in lime saturated water at laboratory temperature of 20 °C and (ii) 72 h curing at a temperature of 60 °C with relative humidity of 90%; (iii) curing at 100% relative humidity until the testing day.

2.2 Characterization tests

Flow-table test. The flow-table test was conducted with the apparatus from ASTM C230 [30]. The test consists of pouring the fresh concrete in the flow mold on the flow table and measuring the concrete diameter as an average of the largest and the smallest diameters (D1 and D2)**.** PVA and STEEL-G1 average flow diameter decrease during fiber volume content increase (Figure 1). Mixes with fiber volume content of 4% and 5%, which showed fiber segregation, presented the lowest flow diameter [31]. The amount of

superplasticizer of STEEL-G2 mixes was increased by 17% to keep a constant flow diameter for different fiber volume content. The Figure 2 allows to visually compares the flow diameter for the 4%STEEL-G1 and 4%STEEL-G2 mixes. Then, the 4%STEEL-G2 mix is much more homogenous than the 4%STEEL-G1 one, that highlight the effects of the different casting methods.

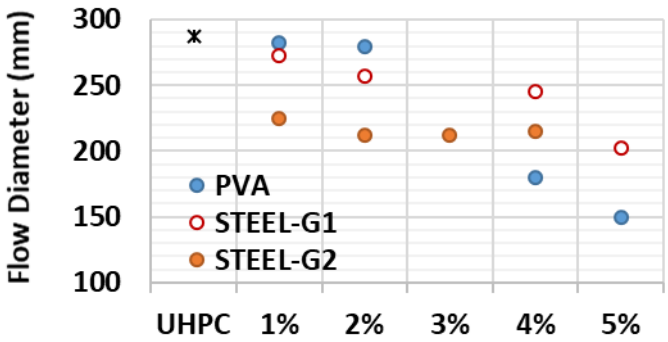

Figure 1. Flow diameter results

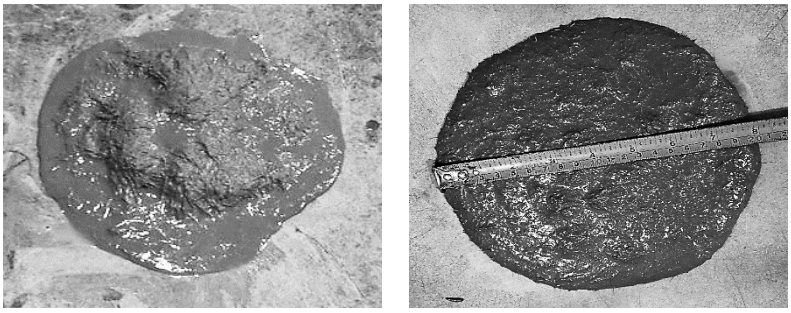

(a) (b)

Figure 2. Visual comparison of the flow-table test results: (a) 4%STEEL-G1 and (b) 4%STEEL-G2

Visual observations. Test cylinders were cut to eliminate both extremities to prevent milt effects. Segregation was observed for UHPFRC-STEEL samples (Figure 3), but not for UHPFRC-PVA. This could be explained by the highest density of steel fibers compared to the PVA ones. Figure 3b shows that more fibers are present on the top of the STEEL-G2 cylinder

compared to the top of the STEEL-G1 cylinder (Figure 3a) meaning that segregation is less important for the G2 mixes. The casting procedure of STEEL-G2, which was without vibration, could explain this fact.

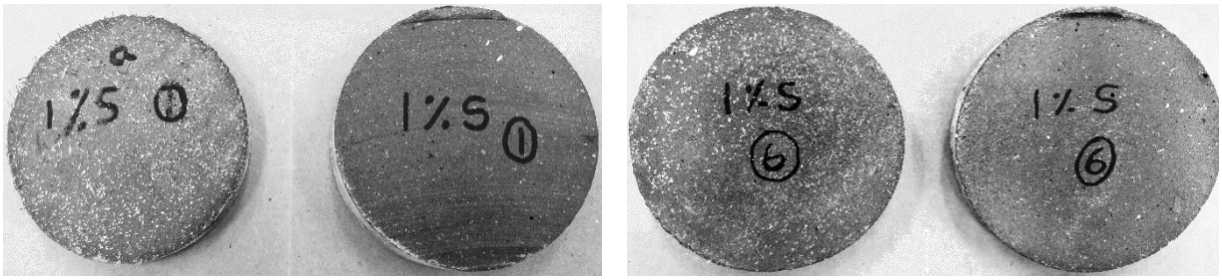

(a) (b)

Figure 3. Bottom (left) and top (right) of the test cylinder for (a) STEEL-G1 samples (b) STEEL-G2 samples

Water porosity. Measures were performed, according to Grandubé [32] and French standard [34], on UHPC, UHPFRC with 1% fiber volume content of steel and PVA (Table 2). UHPFRC-PVA samples were dried at only 50 °C instead of the 110 °C specified by the standard to avoid burning the PVA fibers. Three measurements were performed for each material to ensure the repeatability. All tests were done on samples coming from the center parts of the cylinder to avoid the effect of the observed segregation. These tests were done in order to confirm that the material respect the UHPFRC porosity from the AFGC standard [34].

DRYING TIME	UHPC	UHPFRC 1%PVA	UHPFRC 1%STEEL G1	UHPFRC 1%STEEL G2
6 DAYS	5.6%	4.4%	4.9%	4.4%
2 MONTHS	7.0%	7.6%	7.6%	6.8%

Table 2. Water porosity measurements

After 6 days of drying and no variation of mass for 24 hours, the materials had a water porosity respecting the standard range of UHPC (6 - 9%) and UHPFRC (1.5 - 5%). However, this water porosity procedure is not adapted for this kind of concrete which has very low porosity and

thus, hard to dry in a short delay (24 hours). After the first validation with AFGC recommended value, intervals between mass verification was increased to one week and drying lasted two months. The water porosity results obtained from the extended method revealed less difference between all mixes than the previous results obtain with the recommended method from standards. Water porosity for the STEEL-G2 mixes were lower than the STEEL-G1 mixes, which can be explained by the casting method. Indeed, vibration of G1 mixes may have bonded smaller air bubbles to form bigger ones which are detectable with water porosity measurements.

Mercury Porosity Intrusion (MIP) is effective to quantify the pore distribution from 1 nm up to 100 nm [35]. Analyses were performed for samples of UHPC and UHPFRC with 1% fibers (Figure 4). All tests were done on samples coming from the center parts of the cylinder to avoid the effect of the observed segregation. The pore distributions show similar nanopores (around 2 nm) for all samples. Except for the nanopore of 2 nm, the pore distribution of the different samples shows some differences. For all UHPFRC samples, capillary pores are present between 2 and 50 nm, as opposed to the UHPC samples. The presence of fibers in the material could explain the difference in the pore distribution between the samples with and without fibers. Not only the presence of fibers but the type of fiber as the pore distribution of the PVA samples is different that the STEEL samples. A difference can also be noted from the casting method as STEEL-G1 and STEEL-G2 have different pore distribution between 2 and 50 nm, where STEEL-G2 has a pore distribution more similar to the UHPC one. The variability of the porosity from the casting method can be confirmed from the results of the water porosity where the porosity of the STEEL-G1 and STEEL-G2 are respectively 7.6% and 6.8%. The capillary pores of 20-30 nm for STEEL-G1, which were also observed in the water porosity measures, could influence chloride diffusion and accelerate its migration.

177

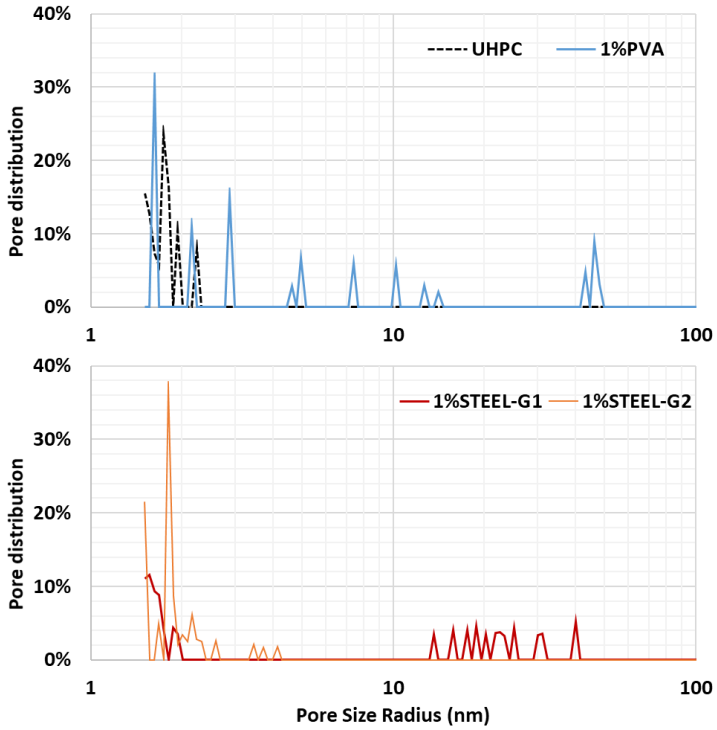

178

179 Figure 4. Pore size distribution between 1 and 100 nm from MIP measures

180 **2.3 Accelerated migration test method**

181 **Samples preparation.** The optimal sample thickness chosen was 25 mm for UHPC and
182 UHPFRC-PVA and 50 mm for UHPFRC-STEEL. The samples were saturated in a water
183 solution with 300 mol/m³ of sodium hydroxide (NaOH) under vacuum pressure for at least
184 16 hours as prescribed in ASTM C1202.

185 **Chloride accelerated migration tests** were carried out according to an adapted protocol of
186 ASTM C1202. The test-set-up for migration tests (Figure 5) was adapted regarding the
187 following points: (i) the volume of the solution was adjusted from 0.5 L to 2.7 L to reduce
188 heating issues; (ii) the voltage was increased from 20V to 70V to accelerate the tests; (iii) the
189 sample thickness was reduced in previous work [31]. After preliminary tests, the sample
190 thickness was chosen to be 50 mm for UHPFRC-STEEL and 25 mm for UHPFRC-PVA and

UHPC. The electrical potential and the duration of the test were 1400 V/m and 28 days respectively. The temperature of the upstream solution, the electrical field passing through the sample and the current were regularly measured.

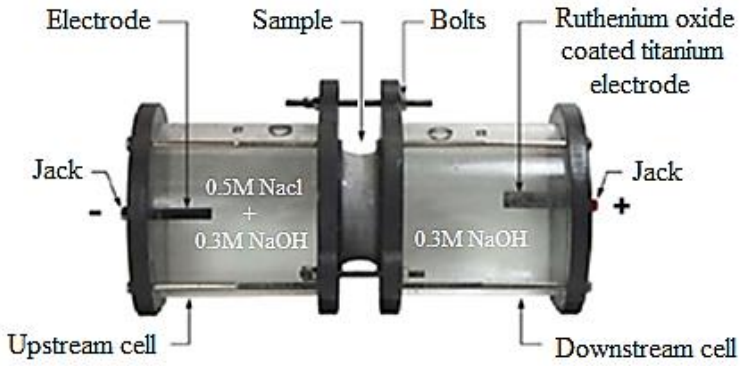

Figure 5. Chloride ion migration cells [11]

Grinding operations were made with a 7.6mm core drill diameter. The concrete powder was collected with a small brush to obtain a minimum of 7.0 g of powder per layers of 1 mm each. The depth of each layer was measured with a caliper. About 10.0 g of concrete powder was collected for each layer.

Chloride titration test. The total chloride present in the concrete powder was extracted with apparel 10% of a nitric acid solution (HNO_3) with a 69% (± 1%) purity. 5 g of concrete powder and 50 ml of acid solution were mixed together. The chloride was extracted through its dissolution, for 1 hour, into the acid. The mixture was then filtered using a vacuum and analyzed by titration with Mettler Toledo T50 titrator.

Transport model. The apparent chloride diffusion coefficient $D_{a,Cl}$ obtained from accelerated chloride migration tests was calculated using the following equation [36]–[38]:

$$D_{a,Cl} = \frac{RTL}{z_{Cl}FU}\left(\frac{x_d - \alpha\sqrt{x_d}}{t}\right). \quad (1)$$

207 R represents the ideal gas constant (83,145 J/mol/K); T the temperature (K); L the thickness of
208 the specimen (m); z the ion valence (z_{Cl} = 1); F the Faraday constant (96,488.46 C/mol), U is
209 the voltage (V); x_d is the chloride penetration depth (mm); t the time test (s) and

$$\alpha = 2\sqrt{\frac{RTL}{zFU}}erf^{-1}\left(1-\frac{2c_d}{c_0}\right), \quad (2)$$

210 where c_d is the chloride concentration (kg/m³) measured at the penetration depth x_d and c_0 is
211 the chloride concentration (kg/m³) at the sample surface.

212 ## 3. RESULTS AND DISCUSSION

213 The migration tests were successfully carried out for all samples of UHPC and UHPFRC-
214 PVA. Moreover, only few samples of UHPFRC-STEEL with a fiber volume content lower than
215 2-3% have passed the test. Most of UHPFRC-STEEL samples presented corrosion and cracks
216 leading to the failure of the accelerated migration test.

217 ### 3.1 Verification of the new accelerated migration test procedure

218 **Resistivity measures.** Considering the applied voltage U (V), the current I (A), the thickness
219 L (m) and the surface S (m²) of the sample, its electrical resistivity ρ (Ω.m) can be obtained
220 with [39]

$$\rho = \frac{U}{I}\frac{S}{L}. \quad (3)$$

221 The resistivity calculated (Figure 6) are very close to each other despite the different the
222 sample thickness used (25 and 50 mm) because the electrical field applied ($E = U/L$) are
223 similar. The samples with fibers presented a lower resistivity than the UHPC one. For the
224 UHPFRC-PVA and STEEL-G1 samples, these results agree with the water porosity measures

225 (∫2.2). The porosity of 1%PVA and 1%STEEL-G1 were greater than the porosity of UHPC
226 samples resulting in a greater ionic quantity in pore solutions, and thus a lower resistivity. The
227 addition of PVA fibers seems linearly proportional to the resistivity of the samples. Despite a
228 lower water porosity for STEEL-G2 compared to the UHPC samples, the STEEL-G2 resistivity
229 was lower. The conductivity of the steel fibers as opposed to the PVA fibers could explain this
230 phenomenon.

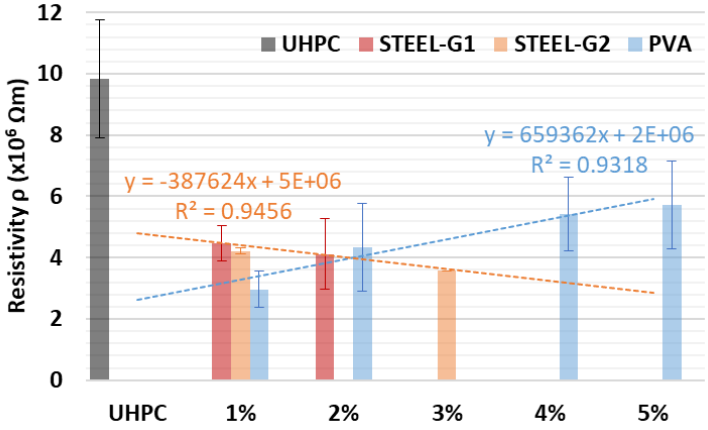

231
232 Figure 6. Initial resistivity of the different samples

233 **Maximal current.** The maximal current (I_{max}) measured during migration tests were
234 between 2 and 13 mA as observed with Figure 7. The current that represent the ionic flux
235 passing through the sample remained very low and did not influence the chloride concentration
236 measures in the first grinded layer (C_1). The applied voltage did not affect the chloride
237 concentration in the first layer as well. In very few cases, the electrode in the downstream cell
238 presented oxidation which required an immediate cleaning to avoid an increase of the resistance
239 and a drop in the electrical potential.

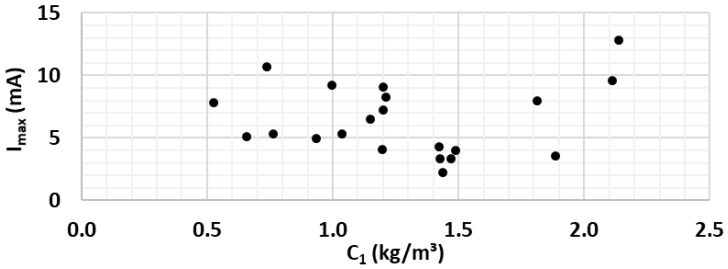

Figure 7. Maximal current measurements according to the chloride concentration at the first grinded layer

Maximal temperature. The current variation did not significantly increase the temperature during the migration tests (Figure 8). Temperature was in between 20 °C and 30 °C which does not involve Joule effects and is much lower than the limit of acceptability (90 °C) of ASTM C1202. These results are in accordance with the expected results for the proposed modifications of the test. A lower electrical field and an augmentation of the volume of the solution allows to keep the temperature at a stable level. For some samples with high-fiber segregation, extensive fiber corrosion was observed. In those cases, the migration test was stopped when the current exceeded 80 mA corresponding to an increase of temperature up to 55 °C. Those last results are not considered in this work.

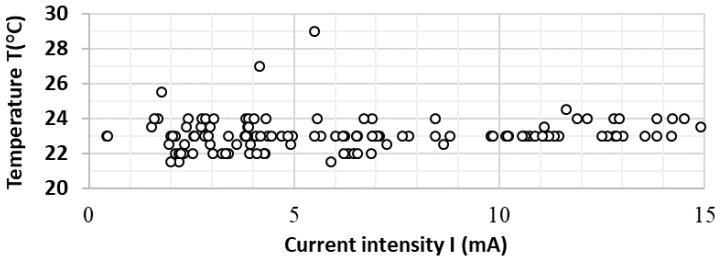

Figure 8. Temperature vs current measurements

3.2 Accelerated migration tests results

Chloride concentration at the surface sample. With the chloride concentration in the upstream cell of C_0 = 500 mol/m³, the maximal chloride mass concentration that could penetrate the concrete pore solution, noted CCE_{max} (kg/m³), is:

$$CCE_{max} = C_0 \cdot M_{Cl} \cdot V_{w/c} \quad (4)$$

where M_{Cl} (35,453 g/mol) is the chloride molar mass and $V_{w/c}$ (m³/m³$_{concrete}$) is the volume of water necessary to cast one cubic meter of concrete. CCE_{max} does not consider hydration reactions during the concrete cure. This calculated upper bound allows to verify the consistency of the results and a possible sample cracking during the migration test. Indeed, all samples with chloride mass concentration higher than the maximal value CCE_{max} have presented signs of cracking. Chloride mass concentrations measured for the first grinded layer (Figure 9) were lower than the maximal value (CCE_{max}). The samples which results are presented in this work did not show any sign of cracking.

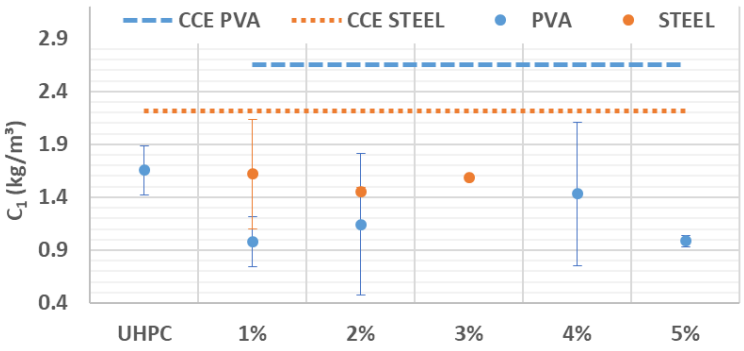

Figure 9. Chloride mass concentration at the first grinded layer

Chloride concentration profiles presented in a first approach gross results of the chloride diffusion in the different materials. The maximum depth reach by chloride is about 5 mm for the UHPC samples (Figure 10). As for UHPFRC, the maximum depth reach is 3.8mm (STEEL-

G1). The two different kinds of fiber (STEEL and PVA) show similar chloride profile except for STEEL-G1 which is slightly higher. STEEL-G2 samples have a higher chloride concentration in the first layer but the penetration depths are lower than the STEEL-G1 samples. The highest chloride concentrations in the first layer grinded are 1.9 kg/m³ for the UHPC and 2.1 kg/m³ for the UHPFRC.

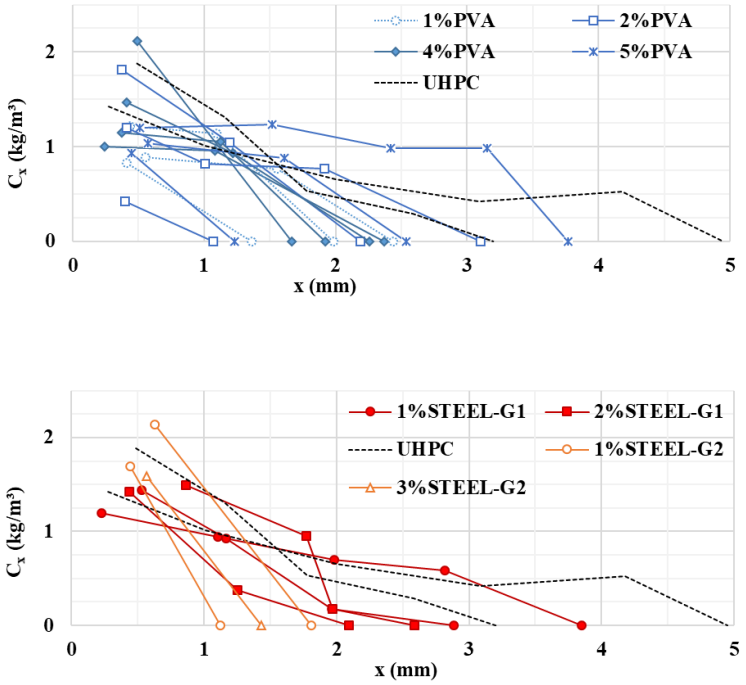

Figure 10. Chloride profile for UHPC, UHPFRC-PVA and UHPFRC-STEEL migration tests

Apparent chloride diffusion coefficient $D_{a,Cl}$ according to the fiber volume. The average diffusion coefficient was calculated using equation (1) for UHPC, UHPFRC-PVA and UHPFRC-STEEL with maximum and minimum values (Figure 11). The quantity of fibers in the sample does not seem to significantly affect the measured diffusion according to the range of the results. Then, median apparent diffusion coefficients and their standard deviations were calculated for the four types of materials regardless the fiber volume (Figure 12). That allows

to have enough samples for each material to realize a statistical analysis and leads to three following conclusions. (i) Considering the water porosity obtain for the different material (Table 2), UHPC has one of the lowest porosities. The expected diffusion coefficient for UHPC should then be inferior or equal to UHPFRC ones, however, the results presented revealed that chloride migration through UHPC is around five times higher than in STEEL-G2 and PVA. That clearly demonstrates the influence of fibers on the chloride diffusion $D_{a,Cl}$ and the importance to consider fibers in durability analyses. Nevertheless, that is not possible to observe a difference between PVA and steel fibers in regard of the uncertainties. (ii) Pore size distribution results with MIP also revealed additional capillarity pores for STEEL-G1 samples (Figure 4) that could accelerate the chloride diffusion and explained a higher $D_{a,Cl}$ than STEEL-G2 ones. The casting method for steel fiber samples hence influence chloride diffusion.

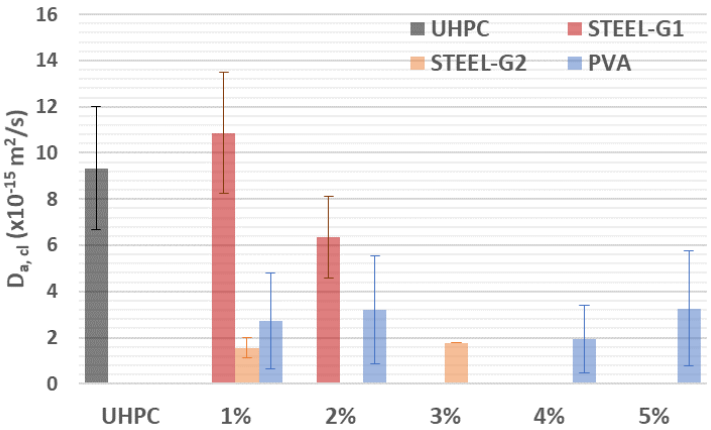

Figure 11. Chloride apparent diffusion coefficient calculated for the different samples

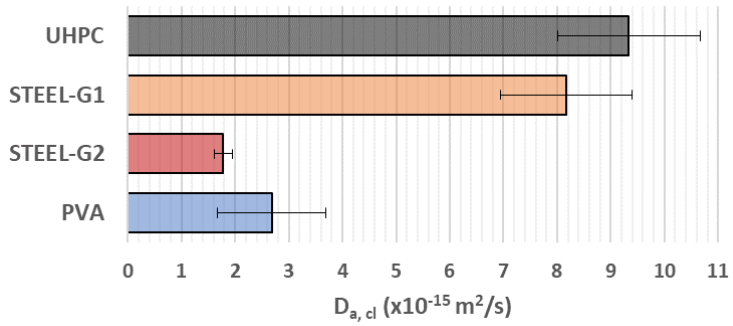

Figure 12. Median apparent diffusion coefficient calculated and its standard deviation according to the type of material

Furthermore, all the diffusion coefficients obtained are in the range of 10^{-14} to 10^{-15} m²/s which is very low compared to diffusion coefficients for ordinary concrete, about 10^{-11} to 10^{-12} m^2/s with an usual w/c ratio (0.35-0.60) [37]. As stated from Table 1, the results from different studies do not highlight significant difference for material with and without fibers according to the ASTM C1202 standard. However, other studies (Table 1) reveals some differences with and without fiber samples by natural diffusion tests. The results from this work confirm the assumption that the standard procedure from ASTM C1202 is insufficient to characterize the material with fiber (UHPFRC) since the presence of fiber does influence the durability of the material. Moreover, the diffusion coefficient of UHPFRC obtain from this work are in accordance with the results from Tanaka [27] for a 5-year chloride exposure. Therefore, this work clearly demonstrates that the proposed procedure test yields accurate diffusion coefficients in a shorter time: 28-days accelerated migration against 5-year chloride exposure.

4. Conclusions

The aim of this work was to propose an alternative test method to ASTM C1202 in order to (i) better characterize the resistance of chloride ion penetration in UHPFRC; and (ii) compare

318 the resistance of chloride ion penetration between UHPC and UHPFRC with two different types
319 of fibers and volume content. The effect of different preparation methods for samples with steel
320 fibers was also considered. The proposed test modifications for the accelerated migration test
321 consisted of (i) increasing the solution volume to reduce heating issues and (ii) the electrical
322 field applied to accelerate the time test; (iii) reducing the sample thickness. The resistivity of
323 the different samples is similar despite variation in their length.

324 All samples had a chloride mass concentration lower than the maximal value expected
325 (CCE_{max}) except for those presenting cracks where the chloride concentration was higher.

326 The procedure for the water porosity was also adapted to obtain more accurate results for
327 UHPC and UHPFRC samples because of their very low porosity.

328 Based on the presented results, the following conclusions can be drawn:

329 • The diffusion results clearly demonstrate that fibers slow down the chloride diffusion in
330 UHPFRC samples.
331 • The casting method for UHPFRC with steel fibers (G1 and G2) has also an influence on
332 the chloride diffusion.
333 • The results from this work are in accordance with the diffusion coefficient obtained with
334 natural diffusion tests from the literature, however, they were obtained in a shorter time
335 which confirms the accuracy of the proposed accelerated test method.

336 Further adaptation on the test set-up is so needed to avoid the issue of corrosion and cracks
337 of steel samples with high fibers volume content. Due to segregation, the steel fiber
338 concentration can be higher in some samples. That leads to a rise of temperature and current
339 during testing. An investigation for a more appropriate method is necessary to obtain an

effective diffusion coefficient and distinguish the influence of the material geometry, the fibers influence and the chloride chemical adsorption.

Acknowledgements

We would like to thank the Natural Sciences and Engineering Research Council of Canada (NSERC), Mitacs, Ministry of transport of Québec and Research Center on Concrete Infrastructure (CRIB) for the financial support and Guillaume Blais-Dufour, Michael Steves Tchuitcheu Tientcheu and Meriem Dhouib for their help during the experimental tests. Finally, we would like to thank Dr. Dominique Corvez of Lafarge Holcim North America for the material donation.

References

[1] A. E. Naaman and K. Wille, 'The path to ultra-high performance fiber reinforced concrete (UHP-FRC): five decades of progress', presented at the Proceeding of 3rd International Symposium on UHPC and Nanotechnology for High Performance Construction Materials. Kassel: Kassel University Press, 2012, pp. 3–13.

[2] E. Fehling, M. Schmidt, J. Walraven, T. Leutbecher, and S. Fröhlich, Eds., '4. Durability', in *Ultra-High Performance Concrete UHPC - Fundamentals, Design, Examples*, Wilhelm Ernst & Sohn, Verlag für Architektur und technische Wissenschaften GmbH & Co. KG, 2014, pp. 59–64.

[3] T. Teichmann and M. Schmidt, 'Influence of the packing density of fine particles on structure, strength and durability of UHPC', in *First international symposium on ultra high performance concrete, Kassel*, 2004, pp. 313–323.

[4] L. Sorelli, G. Constantinides, F.-J. Ulm, and F. Toutlemonde, 'The nano-mechanical signature of ultra high performance concrete by statistical nanoindentation techniques', *Cem. Concr. Res.*, vol. 38, no. 12, pp. 1447–1456, 2008.

[5] F. de Larrard and T. Sedran, 'Optimization of ultra-high-performance concrete by the use of a packing model', *Cem. Concr. Res.*, vol. 24, no. 6, pp. 997–1009, 1994.

[6] E. Denarié and E. Brühwiler, 'Cast-on site UHPFRC for improvement of existing structures–achievements over the last 10 years in practice and research', in *7th workshop on High Performance Fiber Reinforced Cement Composites, 1-3, June 2015, Stuttgart, Germany*, 2015.

[7] E. Brühwiler, '"Structural UHPFRC" : Welcome to the post-concrete era !', presented at the First International Interactive Symposium on UHPC - 2016, 2016.

[8] J. P. Broomfield, *Corrosion of steel in concrete: understanding, investigation and repair*. CRC Press, 2003.

[9] A. Ouglova, Y. Berthaud, F. Foct, M. François, F. Ragueneau, and I. Petre-Lazar, 'The influence of corrosion on bond properties between concrete and reinforcement in concrete structures', *Mater. Struct.*, vol. 41, no. 5, pp. 969–980, 2008.
[10] K. A. T. Vu and M. G. Stewart, 'Structural reliability of concrete bridges including improved chloride-induced corrosion models', *Struct. Saf.*, vol. 22, no. 4, pp. 313–333, 2000.
[11] D. Conciatori, É. Grégoire, É. Samson, J. Marchand, and L. Chouinard, 'Statistical analysis of concrete transport properties', *Mater. Struct.*, vol. 47, no. 1–2, pp. 89–103, Nov. 2014.
[12] T. Stengel and P. Schießl, 'Sustainable construction with UHPC–from life cycle inventory data collection to environmental impact assessment', in *Proceedings of the 2nd international symposium on ultra high performance concrete. Kassel University Press, Kassel*, 2008, pp. 461–468.
[13] S. Piotrowski and M. Schmidt, 'Life cycle cost analysis of a UHPC-bridge on example of two bridge refurbishment designs', in *Proceedings of the 3rd international symposium on ultra-high performance concrete and nanotechnology for high performance construction materials, Kassel*, 2012, pp. 957–964.
[14] M. Thomas, B. Green, E. O'Neal, V. Perry, S. Hayman, and A. Hossack, 'Marine performance of UHPC at Treat Island', presented at the Proceedings of Hipermat 2012 3rd International Symposium on UHPC and Nanotechnology for High Performance Construction Materials, 2012, pp. 365–370.
[15] T. M. Ahlborn, D. L. Misson, E. J. Peuse, and C. G. Gilbertson, 'Durability and Strengh Characterization of Ultre-High Performance Concrete under Variable Curing Regimes', presented at the Second International Symposium on Ultra High Performance Concrete Kassel, Germany March 05-07, 2008, 2008, pp. 197–204.
[16] B. A. Graybeal, 'Material property characterization of ultra-high performance concrete', 2006.
[17] B. A. Graybeal and J. Tanesi, 'Durability of an Ultrahigh-Performance Concrete', *J. Mater. Civ. Eng.*, Oct. 2007.
[18] T. Luping and L.-O. Nilsson, 'Rapid determination of the chloride diffusivity in concrete by applying an electric field', *Mater. J.*, vol. 89, no. 1, pp. 49–53, 1993.
[19] 'Standard Test Method for Electrical Indication of Concrete's Ability to Resist Chloride Ion Penetration', 18.
[20] 'Standard Practice for Fabricating and Testing Specimens of Ultra-High Performance Concrete', 17.
[21] K. Habel, J.-P. Charron, S. Braike, R. D. Hooton, P. Gauvreau, and B. Massicotte, 'Ultra-high performance fibre reinforced concrete mix design in central Canada', *Can. J. Civ. Eng.*, vol. 35, no. 2, pp. 217–224, Feb. 2008.
[22] M. L. Olivier Bonneau Eric Dallaire, Jerome Dugat, and Pierre-Claude Aitcin, 'Mechanical Properties and Durability of Two Industrial Reactive Powder Concretes', *Mater. J.*, vol. 94, no. 4, Jul. 1997.
[23] T. M. Ahlborn, E. J. Peuse, and D. L. Misson, 'Ultra-high-performance-concrete for michigan bridges material performance–phase I', 2008.
[24] 'Standard Test Method for Determining the Apparent Chloride Diffusion Coefficient of Cementitious Mixtures by Bulk Diffusion', 11a 2016.

[25] J. Piérard, B. Dooms, and N. Cauberg, ‘Evaluation of durability parameters of UHPC using accelerated lab tests’, in *Proceedings of the 3rd International Symposium on UHPC and Nanotechnology for High Performance Construction Materials, Kassel, Germany*, 2012, pp. 371–376.
[26] ‘NT Build 443 – Nordtest Method, Accelerated Chloride Penetration’, 1995.
[27] Y. Tanaka, H. Musha, S. Tanaka, and M. Ishida, ‘Durability performance of UFC sakata-mira footbridge under sea environment’, p. 7, 2010.
[28] M. D. Thomas and P. B. Bamforth, ‘Modelling chloride diffusion in concrete: effect of fly ash and slag’, *Cem. Concr. Res.*, vol. 29, no. 4, pp. 487–495, 1999.
[29] ‘ASTM C494.C494M - Chemical Admixtures for Concrete’. ASTM International, 15-Jun-2017.
[30] ‘ASTM C230.C230M - Flow Table for Use in Tests of Hydraulic Cement’. ASTM International, 01-Oct-2014.
[31] G. Blais-Dufour, D. Conciatori, L. Sorelli, and D. Corvez, ‘Modified Chloride Migration Test on UHPFRC Samples’, in *BEFIB 2016*, 2015.
[32] G. Arliguie and H. Hornain, ‘Grandeurs associées à la Durabilité des Bétons’, *Paris Presse L’Ecole Natl. Ponts Chaussées*, 2007.
[33] AFNOR, ‘NF P18-459’, 2010. [Online]. Available: https://www.boutique.afnor.org/norme/nf-p18-459/beton-essai-pour-beton-durci-essai-de-porosite-et-de-masse-volumique/article/707675/fa160729. [Accessed: 22-Mar-2018].
[34] ‘AFGC - Bétons Fibrés à Ultra hautes Performances - Recommandations’. Association Française de Génie Civil, Jun-2013.
[35] S. Diamond, ‘Mercury porosimetry: An inappropriate method for the measurement of pore size distributions in cement-based materials’, *Cem. Concr. Res.*, vol. 30, no. 10, pp. 1517–1525, Oct. 2000.
[36] L. Tong and O. E. Gjørv, ‘Chloride diffusivity based on migration testing’, *Cem. Concr. Res.*, vol. 31, no. 7, pp. 973–982, 2001.
[37] P. Spiesz and H. J. H. Brouwers, ‘Study on the chloride diffusion coefficient in concrete obtained in electrically accelerated tests’, in *Durability of Reinforced Concrete from Composition to Protection*, Springer, 2015, pp. 169–178.
[38] ‘NT Build 492 - Concrete, Mortar and Cement-Based Repair Materials: Chloride Migration Coefficient from Non-Steady-State Migration Experiments’, *Nord. Espoo Finl.*, Nov. 1999.
[39] M. Gussow, *Eletricidade básica: Coleção Schaum*. Bookman Editora, 2009.